Published in final edited form as:

Curr Biol. 2016 May 23; 26(10): 1312–1318. doi:10.1016/j.cub.2016.03.028.

Tropomyosin Promotes Lamellipodial Persistence by Collaborating with Arp2/3 at the Leading Edge

Simon Brayford[1], **Nicole S. Bryce**[1], **Galina Schevzov**[1], **Elizabeth M. Haynes**[2], **James E. Bear**[2], **Edna C. Hardeman**[3], and **Peter W. Gunning**[1,*]

[1]Oncology Research Unit, School of Medical Sciences, UNSW Australia, Sydney, NSW 2052, Australia

[2]Department of Cell and Developmental Biology, University of North Carolina, Chapel Hill, NC 27599-3280, USA

[3]Cellular and Genetic Medicine Unit, School of Medical Sciences, UNSW Australia, Sydney, NSW 2052, Australia

Summary

At the leading edge of migrating cells, protrusion of the lamellipodium is driven by Arp2/3-mediated polymerization of actin filaments [1]. This dense, branched actin network is promoted and stabilized by cortactin [2, 3]. In order to drive filament turnover, Arp2/3 networks are remodelled by proteins such as GMF which blocks the actin-Arp2/3 interaction [4, 5], and coronin 1B which acts by directing SSH1L to the lamellipodium where it activates the actin severing protein cofilin [6, 7]. It has been shown *in vitro* that cofilin-mediated severing of Arp2/3 actin networks results in the generation of new pointed ends to which the actin-stabilizing protein tropomyosin (Tpm) can bind [8]. The presence of Tpm in lamellipodia however is disputed in the literature [9–19]. Here we report that the Tpm isoforms 1.8/9 are enriched in the lamellipodium of fibroblasts as detected with a novel isoform-specific monoclonal antibody. RNAi-mediated silencing of Tpm1.8/9 led to an increase of Arp2/3 accumulation at the cell periphery and a decrease in the persistence of lamellipodia and cell motility, a phenotype consistent with cortactin and coronin 1B-deficient cells [2, 7]. In the absence of coronin 1B or cofilin, Tpm1.8/9 protein levels are reduced while conversely, inhibition of Arp2/3 with CK666 led to an increase in Tpm1.8/9 protein. These findings establish a novel regulatory mechanism within the lamellipodium whereby Tpm collaborates with Arp2/3 to promote lamellipodial-based cell migration.

*Correspondence: p.gunning@unsw.edu.au.

Author contributions

Conceptualization, S.B., P.W.G.; Methodology, S.B., E.M.H., J.E.B.; Investigation, S.B.; Formal Analysis, S.B., N.S.B; Writing – Original Draft, S.B.; Writing – Review & Editing, G.S., N.S.B., E.C.H., P.W.G.; Funding Acquisition and Supervision, G.S., J.E.B., E.C.H., P.W.G.

Results and Discussion

The precise localization of Tpm at the leading edge of cells has been controversial with studies reporting the absence of Tpms from lamellipodia [9–11, 13], and others reporting their presence at or near lamellipodia [16–19]. These opposing observations are partly due to the lack of appropriate reagents to detect the Tpms. Here we report the characterization of a novel monoclonal antibody (α/1b) generated by two overlapping peptides spanning the entire exon 1b of the *Tpm1* gene as the immunogen (Figure 1A). A panel of recombinant Tpm proteins comprised of isoforms representing all four *Tpm* genes was probed with the α/1b antibody. It preferentially detects isoforms Tpm1.8 and Tpm1.9 with minor cross reactivity with Tpm2.1 (Figure 1B). Tpm1.8/9 share a similar amino-terminal exon/intron structure with Tpm1.12 [19], an isoform found at the leading edge of neuronal cells [17]. The spatial distribution of Tpm1.8/9 was assessed in mouse embryonic fibroblasts (MEFs) that display characteristic lamellipodia [20]. MEFs were co-stained with α/1b and CG1 (an antibody specific for Tpm2.1 [19]) in order to demonstrate that lamellipodial staining in these cells is due to the presence of Tpm1.8/9 rather than Tpm2.1, which is more prominent in stress fibers [19, 21, 22]) (Figures 1C and 1D) (see also Figure S1 and S2). MEFs were also co-stained with anti-cortactin and anti-Arp2 to demonstrate that both of these proteins are present in the lamellipodium (Figure 1E), as well as with α/1b and anti-Arp2 (Figure 1F). Finally, 3 μm × 3 μm enlargements (Figure 1G) of regions along the leading edge (indicated in the merge panel of Figure 1F) reveal that, although both are present in the lamellipodium, Tpm1.8/9 (red) and Arp2 (green) do not overlap significantly. Co-localization was quantitated using Pearson's coefficient (Figure 1G), showing that, compared to a cortactin control, Tpm1.8/9 and Arp2 display a significantly lower level of co-localization (R), suggesting that Tpm1.8/9 and Arp2/3 associate with different populations of actin filaments within the lamellipodium. This is supported by *in vitro* studies which showed that binding of the Arp2/3 complex to actin filaments is inhibited by Tpm1.9 [10], but interestingly, not the related Tpm1.12 [17, 23].

Due to the biochemical incompatibility of Arp2/3 and most Tpms, early reports suggested that they were spatially segregated [10, 11]. It has also been proposed that persistent advancement of the cell relies on the underlying lamella [12, 24] which is supported by observations that cell migration is possible without a lamellipodium [13] and Arp2/3 is dispensable for chemotaxis [25]. To investigate the potential role of Tpm1.8/9 in regulating Arp2/3 within the lamellipodium, we designed a siRNA to target exon 1b of the mouse *Tpm1* gene. Western blot analysis of MEF lysates 48 h post transfection shows successful knockdown of Tpm1.8/9 protein (Figure 2A) without impacting other Tpm isoforms (Figure S3). Cells were submitted to a random migration assay, which revealed that Tpm1.8/9 siRNA treated cells exhibited a significant reduction in whole-cell velocity (Figure 2B). Leading edge dynamics was evaluated by generating kymographs of active lamellipodia taken from 10 minute live DIC movies of control or Tpm1.8/9 knockdown MEFs. Analysis of the kymographs revealed that, whilst protrusion velocity (Figure 2C) and retraction velocity (Figure 2D) were both increased as a result of Tpm1.8/9 knockdown, protrusion persistence, a measure of lamellipodial stability, was significantly reduced in Tpm1.8/9 siRNA-treated cells (Figure 2E). Since persistent advancement of the lamellipodium is

largely driven by Arp2/3 activity, and Arp2/3 and Tpm1.8/9 appear to associate with different actin filament populations (Figure 1G), we postulated that Tpm1.8/9 may have an antagonistic effect on the binding of Arp2/3 to actin filaments within the lamellipodium, a property of Tpm1.9 *in vitro* [10]. To test this, we measured the percentage of the cell edge that contains Arp2 relative to cell area in control and Tpm1.8/9 knockdown cells (Figure 2G). Whilst we observed no significant change in cell area (Figure 2F), we saw a significant increase in the percentage of the cell edge that contains Arp2 in the Tpm1.8/9 knockdown cells compared to control (Figure 2H), suggesting that knockdown of Tpm1.8/9 results in an increased ability of the Arp2/3 complex to bind to actin filaments and spread along the cell periphery. Finally, as Arp2/3 activity generates a dense, branched actin network, we hypothesized that its increased activity, due to reduced inhibition from Tpm1.8/9, should also lead to a thicker lamellipodium due to an increased abundance of branched, filamentous actin (F-actin) at the leading edge. The lamellipodium is clearly identifiable as an F-actin rich band, as probed by phalloidin in fibroblasts [26]. We measured the width of the lamellipodium in control and Tpm1.8/9 knockdown cells (Figure 2I). Analysis of 15 cells from each group revealed that lamellipodia in the Tpm1.8/9 knockdown cells were, on average, significantly thicker than those in the control group (Figure 2J).

There is controversy in the literature about the organization of the actin network at the leading edge. Some studies have reported the existence of two spatially segregated zones composed of Arp2/3-branched filaments at the cell edge, and unbranched filaments immediately proximal to this zone [1, 9, 27–29]. Others have stated that these overlap and that both branched and unbranched filaments are present at the very leading edge [30–32]. The formation of a linear array of actin filaments at the leading edge would need to be governed by a precise sequence of appearance of other actin binding proteins following activation of the Arp2/3 complex. Coronin 1B and cofilin have been shown to cooperate to drive the turnover of branched filaments to establish a new network of F-actin [3, 6–8]. To determine whether Tpm1.8/9-containing actin filaments derive from the formation of this F-actin network, the Arp2/3 inhibitor CK666 was used to abolish the lamellipodium. Upon washout of the inihbitor, Arp2/3 activity is rapidly restored and formation of new lamellipodia can be synchronized [33, 34]. We found that after 5 seconds of washout of the inhibitor, Arp2 staining can be seen at the very tips of newly formed lamellipodia (Figure 3A). This is consistent with the well established role of Arp2/3 in the initiation of lamellipodia [13, 23, 25, 35]. Strikingly, Tpm1.8/9 is absent from these structures at this early timepoint. However, after 30 seconds, some enrichment of Tpm1.8/9 is clearly visible at the periphery of cells (Figure 3B). We also examined the timecourse of appearance of other actin binding proteins and found that cortactin is also rapidly recruited following the re-activation of Arp2/3 although not to the same extent as Arp2/3 (Figure 3C). This is also consistent with the role of cortactin in the stabilization of Arp2/3-nucleated filaments at the leading edge [2, 3]. In contrast, significantly fewer cells displayed coronin 1B enrichment at the leading edge at 5 or 10 seconds after CK666 washout, with enrichment seen in the majority of cells after 30 seconds of washout. Collectively, these data indicate that coronin 1B and Tpm1.8/9, while not essential for initiation of lamellipodial protrusion, may play a role in the maintenance and persistence of lamellipodia by generating and stabilizing the F-actin network. Finally cofilin, which is present fairly homogenously throughout the cell,

including the lamellipodium, in both migrating and non-migrating fibroblasts [26], was enriched at the very earliest of timepoints closely following that of Arp2/3. Cofilin is activated via dephosphorylation by protein phosphatase slingshot homolog 1 (SSH1L) which is directed to the lamellipodium by coronin 1B [7]. We postulate that, although cofilin is present in early lamellipodia, it is not until the later recruitment of coronin 1B/SSH1L that cofilin is activated, and begins severing the Arp2/3 network, as has been described in a cell-free system [8].

These findings raise an important question - how can multiple actin filament populations coexist in the same cellular region yet be differentially regulated [17]? It has recently been shown *in vitro* that severing of Arp2/3-generated networks by cofilin results in the generation of new pointed ends to which the *Drosophila*-derived Tpm, Tm1A, preferentially binds, generating two sets of actin filaments. One is Tpm-coated and the other Tpm-free that is competent to bind Arp2/3. They can be stably maintained *in vitro* because they are insulated from each another [8]. These findings point toward a potential mechanism of how branched actin filaments may be re-modelled in cells to include Tpm. Recent experiments indicate the importance of building multiple actin filament types in the same location to generate functional outcomes [36, 37]. Studies in a variety of systems support that Tpm isoforms are used to specify the functional and molecular properties of actin filaments to allow the collaboration of different filament populations within the cell [38]. By a mechanism that is not yet fully understood, Tpm isoforms display extensive sorting, both at a tissue and intracellular level resulting in spatially distinct actin filament populations [22, 39]. Because of the co-recruitment of Tpm1.8/9 and coronin 1B in newly formed lamellipodia, we postulated that coronin 1B and/or active cofilin may be required for Tpm1.8/9 targeting to lamellipodial actin filaments. To test this we used siRNA sequences to knockdown coronin 1B or its downstream effector cofilin and examined Tpm1.8/9 localization using the α/1b antibody. We observed that significantly fewer cells displayed lamellipodial enrichment of Tpm1.8/9 in the coronin 1B (24.6 ± 2.0 %, $p < 0.0001$) and cofilin (16.0 ± 3.3 %, $p < 0.0001$) siRNA knockdown cells compared to control cells (71.3 ± 1.3 %) (images not shown). We hypothesized that the lack of Tpm1.8/9 at the leading edge following the knockdown of coronin 1B or cofilin could potentially be as a result of protein degradation. Western blots of siRNA treated cell lysates demonstrate a significant reduction in the overall levels of Tpm1.8/9 (Figure 4A, upper panel and 4B). As no significant change was observed in the mRNA levels for Tpm1.8/9 as revealed by qPCR (Figure 4E), this effect is likely due to Tpm1.8/9 protein being degraded when it cannot bind as effectively to actin filaments in the lamellipodium. To investigate whether Tpm1.8/9 was being degraded by the 26S proteasome, the proteasome inhibitor MG132 was used. Cells transfected with Coronin 1B or cofilin siRNA were treated with 20μM MG132 for 6 hours. Protein lysates for treated and untreated cells were separated by SDS-PAGE, and blots were probed with the α/1b antibody. The same lysates were later run on a separate gel alongside non-inhibitor treated lysates and probed for Hsp70, a chaperone that is known to be degraded by the 26S proteasome. As expected, the MG132-treated samples showed increased levels of Hsp70 compared to untreated samples (Figure 4A, lower panel). There was no apparent restoration of Tpm1.8/9 protein levels following MG132 treatment (Figure 4A, upper panel) suggesting Tpm1.8/9 is not degraded by the proteasome. In contrast to the result of Coronin 1B/cofilin

knockdown, knockdown of cortactin had no significant impact on the localization ($p = 0.7828$) or protein level ($p = 0.0785$) of Tpm1.8/9 (Figure S4). Finally, we examined the effect of CK666 on Tpm1.8/9 protein levels using a time-course assay and found that after 6 hours exposure to the Arp2/3 inhibitor, Tpm1.8/9 levels were significantly increased compared to DMSO control (Figure 4C and D). Despite an increase in protein level, Tpm1.8/9 is not redistributed to other structures such as stress fibers (Figure S2D). This result further indicates a regulatory relationship between Arp2/3 and Tpm1.8/9 whereby if Tpm1.8/9 is silenced, Arp2/3 activity increases (Figures 2H and 2J) and conversely, if Arp2/3 is inhibited by CK666, Tpm1.8/9 expression is transiently increased (Figures 4C and 4D). This effect is supported by the results outlined in Figure 3 whereby under CK666 inhibition, even though expression is upregulated, Tpm1.8/9 do not have access to the leading edge until Arp2/3 activity is restored and coronin 1B/cofilin remodelling can take place.

The findings of this study may provide a solution to the controversy found in the literature and offer a novel mechanism of how Tpm and Arp2/3 collaborate at the leading edge. At the advancing cell edge, coronin 1B and cofilin coordinate the transition between a network of non-Tpm-containing Arp2/3-branched filaments and a second, Tpm-containing network of linear filaments by generating exposed pointed ends which become coated with Tpm1.8/9. This provides the stability needed to enhance persistence through the subsequent promotion of substratum adhesions. In the absence of coronin 1B, cofilin is not activated and fewer free pointed ends to which Tpm can bind are created. Tpm may be subsequently degraded and therefore depleted from the leading edge, an observation also seen following the knockdown of cofilin. As a result of reduced Tpm levels, the presence of more stable, unbranched filaments is diminished and lamellipodial persistence is impaired. In conclusion, the tropomyosin isoforms Tpm1.8/9 are specifically recruited to the leading edge of migrating cells where they promote the transition from a branched actin network to a more stable actin network in order to achieve a persistent state of lamellipodial protrusion.

Supplementary Material

Refer to Web version on PubMed Central for supplementary material.

Acknowledgments

This work was supported by Project Grant APP1004175 from the Australian National Health and Medical Research Council (NHMRC) (P.W.G, G.S, E.C.H) and funding from The Kids Cancer Project. S.B is the recipient of an Australian Postgraduate Award and is supported by the Translational Cancer Research Network (TCRN), Australia.

References

1. Pollard TD, Borisy GG. Cellular motility driven by assembly and disassembly of actin filaments. Cell. 2003; 112:453–465. [PubMed: 12600310]
2. Bryce NS, Clark ES, Leysath JL, Currie JD, Webb DJ, Weaver AM. Cortactin promotes cell motility by enhancing lamellipodial persistence. Curr Biol. 2005; 15:1276–1285. [PubMed: 16051170]
3. Weaver AM, Karginov AV, Kinley AW, Weed SA, Li Y, Parsons JT, Cooper JA. Cortactin promotes and stabilizes Arp2/3-induced actin filament network formation. Curr Biol. 2001; 11:370–374. [PubMed: 11267876]

4. Poukkula M, Hakala M, Pentinmikko N, Sweeney MO, Jansen S, Mattila J, Hietakangas V, Goode BL, Lappalainen P. GMF promotes leading-edge dynamics and collective cell migration in vivo. Curr Biol. 2014; 24:2533–2540. [PubMed: 25308079]
5. Haynes EM, Asokan SB, King SJ, Johnson HE, Haugh JM, Bear JE. GMFbeta controls branched actin content and lamellipodial retraction in fibroblasts. J Cell Biol. 2015; 209:803–812. [PubMed: 26101216]
6. Cai L, Makhov AM, Schafer DA, Bear JE. Coronin 1B antagonizes cortactin and remodels Arp2/3-containing actin branches in lamellipodia. Cell. 2008; 134:828–842. [PubMed: 18775315]
7. Cai L, Marshall TW, Uetrecht AC, Schafer DA, Bear JE. Coronin 1B coordinates Arp2/3 complex and cofilin activities at the leading edge. Cell. 2007; 128:915–929. [PubMed: 17350576]
8. Hsiao JY, Goins LM, Petek NA, Mullins RD. Arp2/3 Complex and Cofilin Modulate Binding of Tropomyosin to Branched Actin Networks. Curr Biol. 2015; 25:1573–1582. [PubMed: 26028436]
9. Iwasa JH, Mullins RD. Spatial and temporal relationships between actin-filament nucleation, capping, and disassembly. Curr Biol. 2007; 17:395–406. [PubMed: 17331727]
10. Blanchoin L, Pollard TD, Hitchcock-DeGregori SE. Inhibition of the Arp2/3 complex-nucleated actin polymerization and branch formation by tropomyosin. Curr Biol. 2001; 11:1300–1304. [PubMed: 11525747]
11. DesMarais V, Ichetovkin I, Condeelis J, Hitchcock-DeGregori SE. Spatial regulation of actin dynamics: a tropomyosin-free, actin-rich compartment at the leading edge. J Cell Sci. 2002; 115:4649–4660. [PubMed: 12415009]
12. Ponti A, Machacek M, Gupton SL, Waterman-Storer CM, Danuser G. Two distinct actin networks drive the protrusion of migrating cells. Science. 2004; 305:1782–1786. [PubMed: 15375270]
13. Gupton SL, Anderson KL, Kole TP, Fischer RS, Ponti A, Hitchcock-DeGregori SE, Danuser G, Fowler VM, Wirtz D, Hanein D, et al. Cell migration without a lamellipodium: translation of actin dynamics into cell movement mediated by tropomyosin. J Cell Biol. 2005; 168:619–631. [PubMed: 15716379]
14. Skau CT, Plotnikov SV, Doyle AD, Waterman CM. Inverted formin 2 in focal adhesions promotes dorsal stress fiber and fibrillar adhesion formation to drive extracellular matrix assembly. Proc Natl Acad Sci U S A. 2015; 112:E2447–2456. [PubMed: 25918420]
15. Koestler SA, Steffen A, Nemethova M, Winterhoff M, Luo N, Holleboom JM, Krupp J, Jacob S, Vinzenz M, Schur F, et al. Arp2/3 complex is essential for actin network treadmilling as well as for targeting of capping protein and cofilin. Mol Biol Cell. 2013; 24:2861–2875. [PubMed: 23885122]
16. Lin JJ, Hegmann TE, Lin JL. Differential localization of tropomyosin isoforms in cultured nonmuscle cells. J Cell Biol. 1988; 107:563–572. [PubMed: 3047141]
17. Bryce NS, Schevzov G, Ferguson V, Percival JM, Lin JJ, Matsumura F, Bamburg JR, Jeffrey PL, Hardeman EC, Gunning P. Specification of actin filament function and molecular composition by tropomyosin isoforms. Mol Biol Cell. 2003; 14:1002–1016. [PubMed: 12631719]
18. Hillberg L, Zhao Rathje LS, Nyakern-Meazza M, Helfand B, Goldman RD, Schutt CE, Lindberg U. Tropomyosins are present in lamellipodia of motile cells. Eur J Cell Biol. 2006; 85:399–409. [PubMed: 16524642]
19. Schevzov G, Whittaker SP, Fath T, Lin JJ, Gunning PW. Tropomyosin isoforms and reagents. Bioarchitecture. 2011; 1:135–164. [PubMed: 22069507]
20. Coombes J, Schevzov G, Kan C-Y, Petti C, Maritz MF, Whittaker S, MacKenzie KL, Gunning PW. Ras transformation overrides a proliferation defect induced by Tpm3.1 knockout. Cell Mol Biol Lett. 2015; 20:4.
21. Temm-Grove CJ, Jockusch BM, Weinberger RP, Schevzov G, Helfman DM. Distinct localizations of tropomyosin isoforms in LLC-PK1 epithelial cells suggests specialized function at cell-cell adhesions. Cell Motil Cytoskeleton. 1998; 40:393–407. [PubMed: 9712268]
22. Schevzov G, Vrhovski B, Bryce NS, Elmir S, Qiu MR, O'Neill GM, Yang N, Verrills NM, Kavallaris M, Gunning PW. Tissue-specific tropomyosin isoform composition. J Histochem Cytochem. 2005; 53:557–570. [PubMed: 15872049]
23. Kis-Bicskei N, Vig A, Nyitrai M, Bugyi B, Talian GC. Purification of tropomyosin Br-3 and 5NM1 and characterization of their interactions with actin. Cytoskeleton (Hoboken). 2013; 70:755–765. [PubMed: 24124168]

24. Lim JI, Sabouri-Ghomi M, Machacek M, Waterman CM, Danuser G. Protrusion and actin assembly are coupled to the organization of lamellar contractile structures. Exp Cell Res. 2010; 316:2027–2041. [PubMed: 20406634]
25. Wu C, Asokan SB, Berginski ME, Haynes EM, Sharpless NE, Griffith JD, Gomez SM, Bear JE. Arp2/3 is critical for lamellipodia and response to extracellular matrix cues but is dispensable for chemotaxis. Cell. 2012; 148:973–987. [PubMed: 22385962]
26. Dawe HR, Minamide LS, Bamburg JR, Cramer LP. ADF/cofilin controls cell polarity during fibroblast migration. Curr Biol. 2003; 13:252–257. [PubMed: 12573223]
27. Svitkina TM, Verkhovsky AB, McQuade KM, Borisy GG. Analysis of the actin-myosin II system in fish epidermal keratocytes: mechanism of cell body translocation. J Cell Biol. 1997; 139:397–415. [PubMed: 9334344]
28. Svitkina TM, Borisy GG. Arp2/3 complex and actin depolymerizing factor/cofilin in dendritic organization and treadmilling of actin filament array in lamellipodia. J Cell Biol. 1999; 145:1009–1026. [PubMed: 10352018]
29. Vallotton P, Small JV. Shifting views on the leading role of the lamellipodium in cell migration: speckle tracking revisited. J Cell Sci. 2009; 122:1955–1958. [PubMed: 19494123]
30. Urban E, Jacob S, Nemethova M, Resch GP, Small JV. Electron tomography reveals unbranched networks of actin filaments in lamellipodia. Nat Cell Biol. 2010; 12:429–435. [PubMed: 20418872]
31. Vinzenz M, Nemethova M, Schur F, Mueller J, Narita A, Urban E, Winkler C, Schmeiser C, Koestler SA, Rottner K, et al. Actin branching in the initiation and maintenance of lamellipodia. J Cell Sci. 2012; 125:2775–2785. [PubMed: 22431015]
32. Small JV. Pushing with actin: from cells to pathogens. Biochem Soc Trans. 2015; 43:84–91. [PubMed: 25619250]
33. Liu Z, Yang X, Chen C, Liu B, Ren B, Wang L, Zhao K, Yu S, Ming H. Expression of the Arp2/3 complex in human gliomas and its role in the migration and invasion of glioma cells. Oncol Rep. 2013; 30:2127–2136. [PubMed: 23969835]
34. Nolen BJ, Tomasevic N, Russell A, Pierce DW, Jia Z, McCormick CD, Hartman J, Sakowicz R, Pollard TD. Characterization of two classes of small molecule inhibitors of Arp2/3 complex. Nature. 2009; 460:1031–1034. [PubMed: 19648907]
35. Bailly M, Macaluso F, Cammer M, Chan A, Segall JE, Condeelis JS. Relationship between Arp2/3 complex and the barbed ends of actin filaments at the leading edge of carcinoma cells after epidermal growth factor stimulation. J Cell Biol. 1999; 145:331–345. [PubMed: 10209028]
36. Kee AJ, Yang L, Lucas CA, Greenberg MJ, Martel N, Leong GM, Hughes WE, Cooney GJ, James DE, Ostap EM, et al. An actin filament population defined by the tropomyosin Tpm3.1 regulates glucose uptake. Traffic. 2015; 16:691–711. [PubMed: 25783006]
37. Tojkander S, Gateva G, Schevzov G, Hotulainen P, Naumanen P, Martin C, Gunning PW, Lappalainen P. A molecular pathway for myosin II recruitment to stress fibers. Curr Biol. 2011; 21:539–550. [PubMed: 21458264]
38. Gunning PW, Hardeman EC, Lappalainen P, Mulvihill DP. Tropomyosin - master regulator of actin filament function in the cytoskeleton. J Cell Sci. 2015; 128:2965–2974. [PubMed: 26240174]
39. Martin C, Gunning P. Isoform sorting of tropomyosins. Adv Exp Med Biol. 2008; 644:187–200. [PubMed: 19209823]

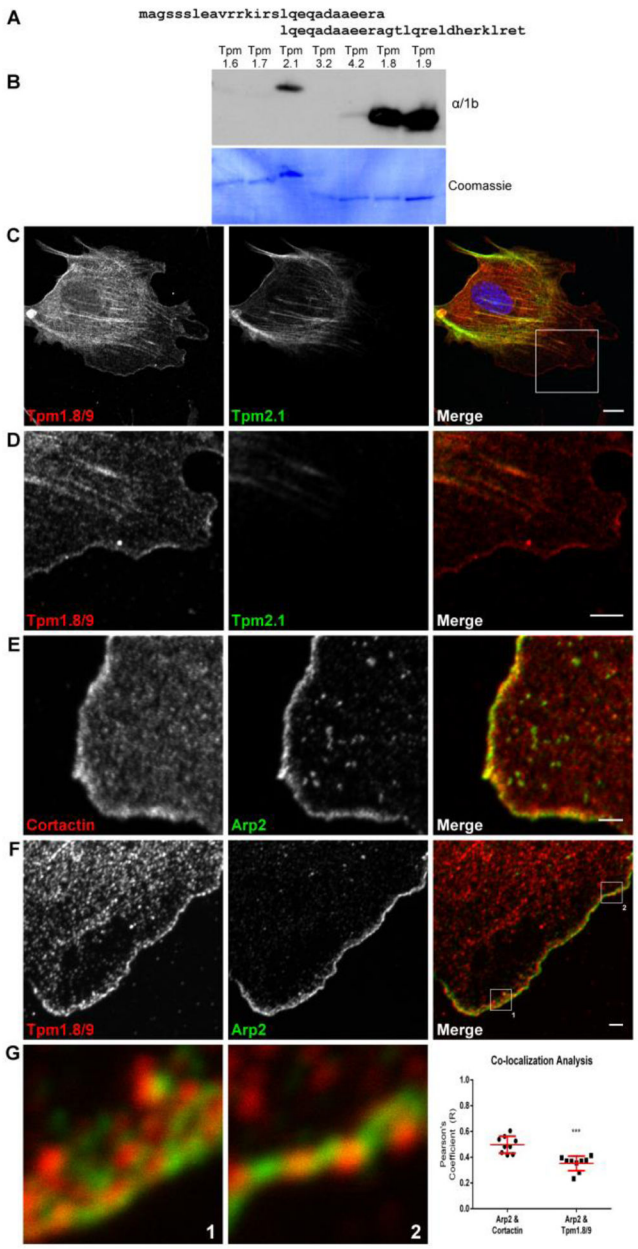

Figure 1. The Tpm isoforms 1.8/9 are enriched in the lamellipodium of fibroblasts as detected with a novel isoform-specific monoclonal antibody (See also Figures S1 and S2)

(A) Peptides that span the entire exon 1b of the *Tpm1* gene were used as the immunogen to generate the rat α/1b monoclonal antibody.

(B) Western blot of recombinant Tpm isoforms showing isoform specificity of the α/1b antibody for Tpm1.8 and Tpm1.9 with minor cross-reactivity with Tpm2.1.

(C) Representative confocal image of a MEF cell co-stained for Tpm1.8/9 and Tpm2.1, demonstrating that only Tpm1.8/9 are present in the lamellipodium. Merged image shows Tpm1.8/9 in red, Tpm2.1 in green and nucleus stain with DAPI (blue). Scale bar = 10 μm. See also Figure S1.

(D) 30 μm × 30 μm enlargement of the boxed region in (C, merge) showing, in detail, the presence of Tpm1.8/9 and absence of Tpm2.1 from the lamellipodium. Scale bar = 5 μm.
(E) 5x magnification of the lamellipodium of a MEF cell co-stained for cortactin and Arp2, used as a control to demonstrate that both of these proteins occupy the lamellipodium. Merged image shows cortactin in red and Arp2 in green Scale bar = 2 μm.
(F) 3x magnification of the lamellipodium of a MEF cell co-stained for Tpm1.8/9 and Arp2 to demonstrate that both of these proteins occupy the lamellipodium. Merged image shows Tpm1.8/9 in red and Arp2 in green Scale Bar = 2 μm.
(G) 3 μm × 3 μm enlargements of the regions shown in the merge panel from (E), showing that, although both present in the lamellipodium, Tpm1.8/9 (red) and Arp2 (green) do not strongly overlap. This is demonstrated quantitatively by co-localization analysis of the images by Pearson's coefficient, where compared to cortactin control (individual zooms not shown), Tpm1.8/9 and Arp2 display a significantly lower level of co-localization (R). Error bars ± SEM; n = 9; ***$p < 0.001$; Student's t-test.

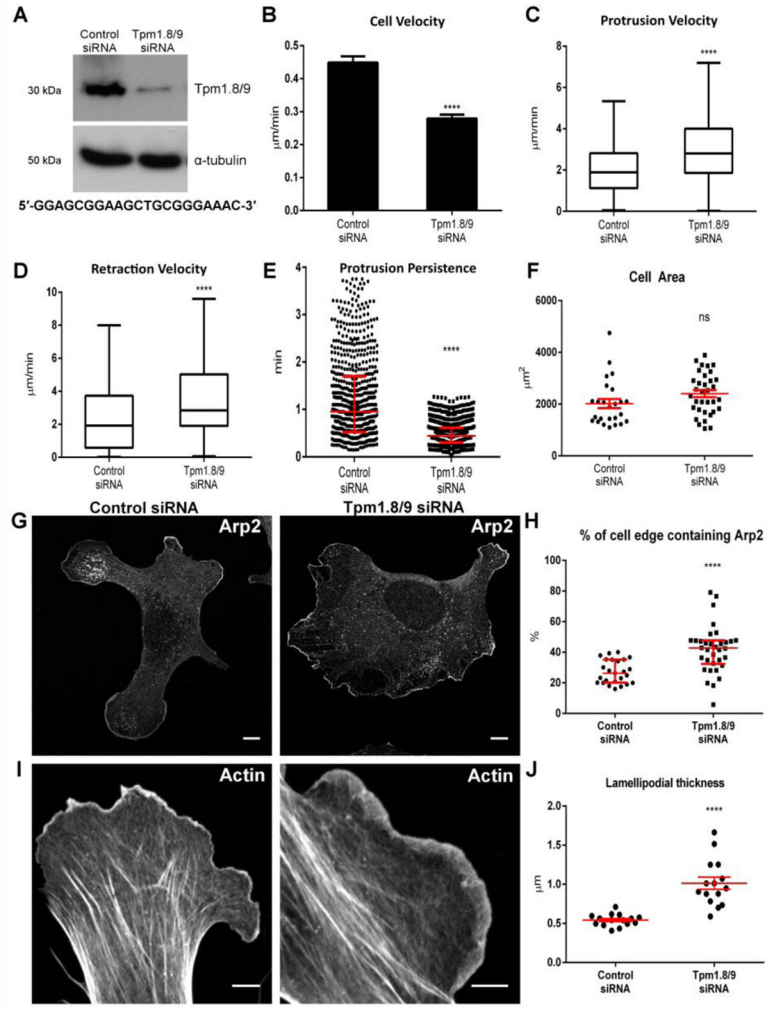

Figure 2. RNAi-mediated silencing of Tpm1.8/9 results in reduced in cell speed and lamellipodial persistence and leads to an increase of Arp2/3 accumulation at the cell periphery and (See also Figure S3)

(A) Western blot showing Tpm1.8/9 expression in MEFs 48 h post transfection with either control (non-silencing) or Tpm1.8/9 siRNA. α-tubulin was used as a loading control. Target sequence shown below blot.

(B) Histogram showing average (control, n = 79 cells; Tpm1.8/9 siRNA, n = 74 cells) cell velocity. Error bars = SEM; n = 4, ****p < 0.0001; Student's t-test.

(C & D) Quantitation of kymographs (control, n = 228 kymographs generated for 30 cells; Tpm1.8/9 siRNA, n = 181 kymographs generated for 23 cells) showing the velocity of protrusions (C) and retractions (D). For Tukey box plots, whiskers indicate maximum and minimum values within 1.5 IQR, the box represents the 25th–75th quartile, and the line indicates the median. n = 4; ****p < 0.0001; Student's *t*-test.

(E) Quantitation of kymographs showing protrusion persistence in Tpm1.8/9 treated cells compared to control siRNA treated cells. Error bars ± SEM; Control siRNA, n = 228 kymographs generated for 30 cells; Tpm1.8/9 siRNA, n = 181 kymographs generated for 23 cells; ****p < 0.0001; Student's t-test.

(F) Quantitation of image analysis showing no significant difference in cell area in control siRNA compared to Tpm1.8/9 siRNA treated cells. Error bars ± SEM; n = 25; ns = not statistically significant; Student's t-test.
(G) MEFs stained for Arp2, 48 h post transfection with either control (left) or Tpm1.8/9 siRNA (right). Scale bars = 10 μm.
(H) Quantitation of image analysis showing % of cell edge containing Arp2 is significantly increased in the knockdowns. Error bars ± SEM; n = 25; ****p < 0.0001; Student's t-test.
(I) MEFs stained with Phalloidin, 48 h post transfection with either control (left, 2.0 x magnification) or Tpm1.8/9 siRNA (right, 2.6 x magnification). Scale bars = 5 μm.
(J) Quantitation of image analysis showing lamellipodial thickness is significantly increased in Tpm1.8/9 knockdown cells. Error bars ± SEM; n = 15; ****p < 0.0001; Student's t-test.

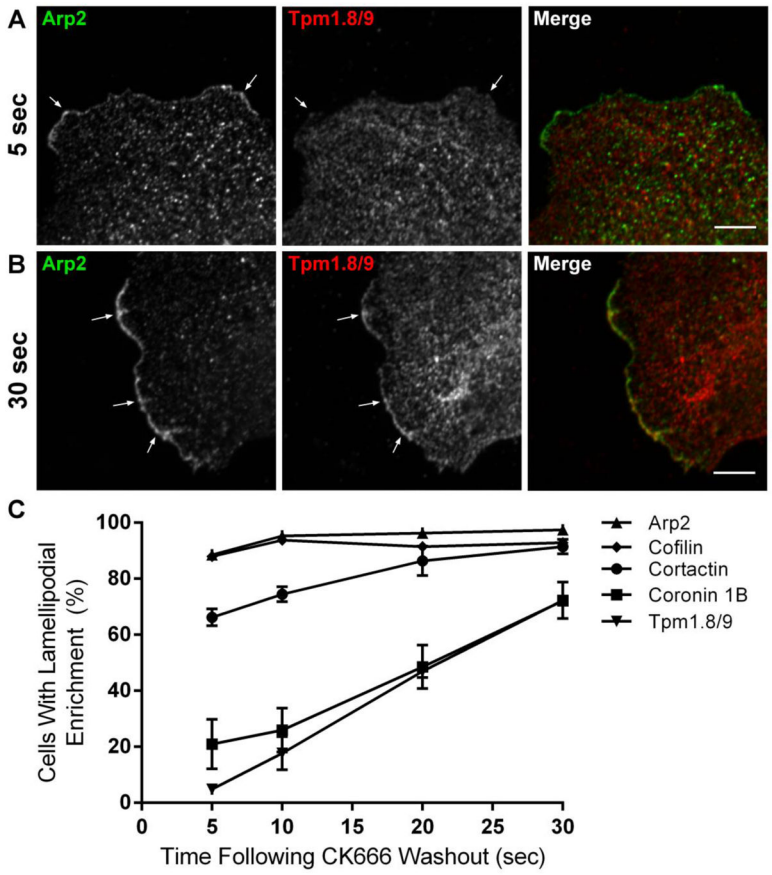

Figure 3. Sequence of appearance of other actin binding proteins following activation of the Arp2/3 complex

Cells were treated with the Arp2/3 inhibitor CK666 at 150 μM for 3 hr, the inhibitor was then washed out and cells fixed at 5, 10, 20 or 30 sec.

(A) Representative confocal image of a newly formed lamellipodium in a MEF cell (3 x magnification), co-stained for Arp2 (green) and Tpm1.8/9 (red) at 5 seconds following washout of CK666. Scale bar = 5 μm.

(B) Representative confocal image of a newly formed lamellipodium in a MEF cell (3 x magnification), co-stained for Arp2 (green) and Tpm1.8/9 (red) at 30 seconds following washout of CK666. Scale bar = 5 μm.

(C) Quantitation shown as a percentage of cells displaying lamellipodial enrichment of the relevant protein at the various time-points following drug washout; Error bars ± SEM; n > 100 cells per antibody per time-point. n = 3.

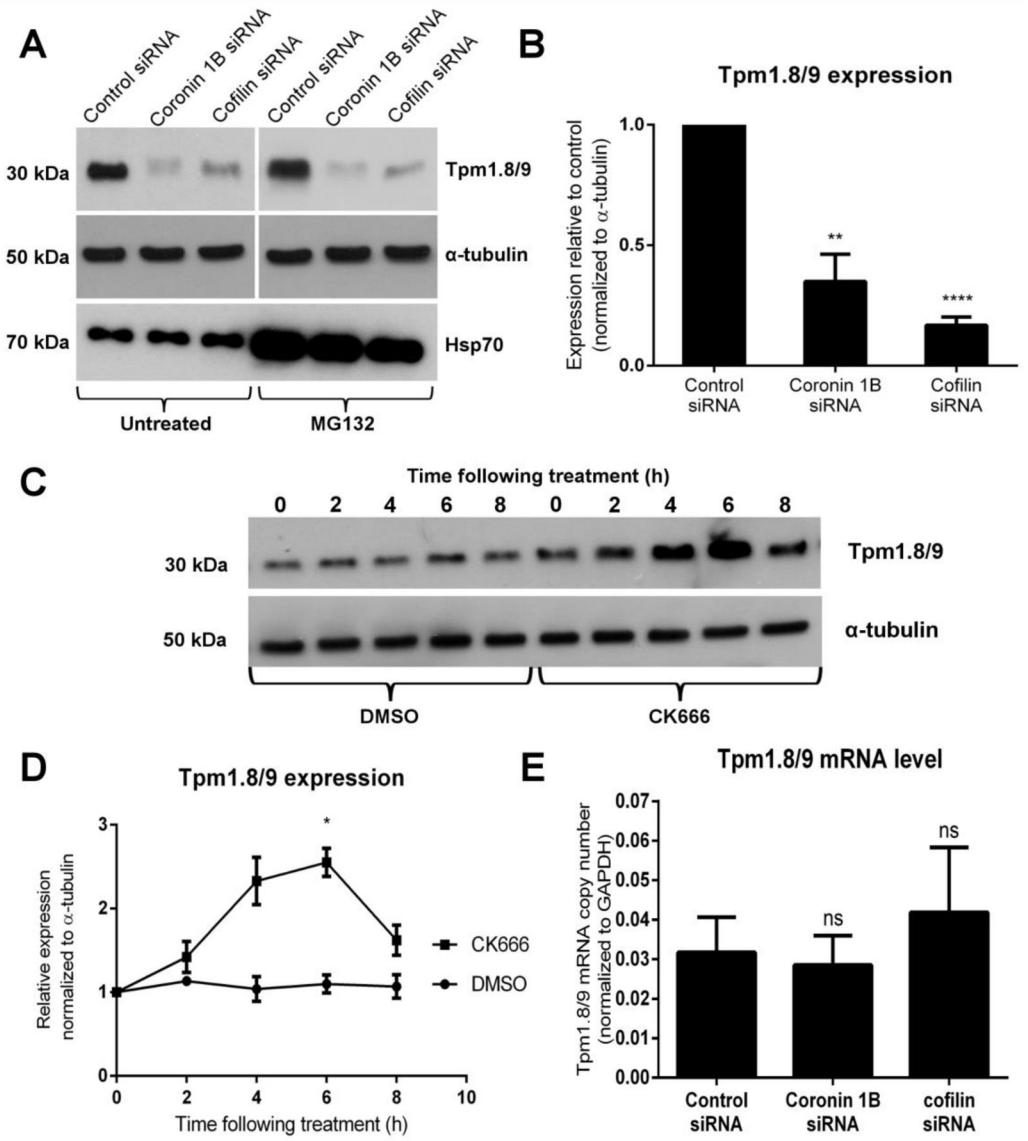

Figure 4. In the absence of coronin 1B or cofilin, Tpm1.8/9 protein levels are reduced while conversely, inhibition of Arp2/3 with CK666 leads to an increase in Tpm1.8/9 protein (see also Figures S2 and S4)

(A) Western blot showing degradation of Tpm1.8/9 protein following siRNA knockdown of either coronin 1B or cofilin compared to control siRNA (top panel, left) with α-tubulin as a loading control (middle panel). Treatment with proteasome inhibitor MG132 does not restore Tpm1.8/9 protein levels (top panel, right). The same lysates from the upper panels were run together on a separate gel and probed for Hsp70 as a positive control to demonstrate successful inhibition of the proteasome (lower panel, right) compared to lysates from untreated cells (lower panel, left).

(B) Quantitation of western blots showing a significant reduction in Tpm1.8/9 protein levels (normalized to α-tubulin) following siRNA knockdown of coronin 1B or cofilin compared to control; Error bars = SEM; n = 3; **p<0.01, ****p < 0.0001; Student's t-test.

(C) Western blot showing Tpm1.8/9 protein levels at 2 h time points following CK666 treatment compared to DMSO vehicle control. α-tubulin was used as a loading control.
(D) Quantitation of western blots in (C) showing an increase in Tpm1.8/9 protein levels (normalized to α-tubulin) post-CK666 treatment with a statistically significant increase at 6 h post-treatment. Error bars ± SEM; n = 3; *$p<0.05$; Student's t-test.
(E) qPCR analysis of Tpm1.8/9 mRNA taken from cDNA generated from either control, coronin 1B or cofilin siRNA treated cells; Error bars = SEM; n = 2; ns = not statistically significant; Student's t-test.